

THE CHOICE OF DIVERGENCE: A NEGLECTED KEY TO MITIGATING DIVERSITY COLLAPSE IN REINFORCEMENT LEARNING WITH VERIFIABLE REWARD

Long Li¹, Jiaran Hao¹, Jason Klein Liu¹, Zhijian Zhou², Yanting Miao⁴, Wei Pang⁴,

Xiaoyu Tan¹, Wei Chu¹, Zhe Wang³, Shirui Pan³, Chao Qu^{1,2*}, Yuan Qi^{1,2}

¹INFLY TECH, ²Fudan University, ³Griffith University, ⁴University of Waterloo

{seamoke111@gmail.com}

 github.com/seamoke/DPH-RL

ABSTRACT

A central paradox in fine-tuning Large Language Models (LLMs) with Reinforcement Learning with Verifiable Reward (RLVR) is the frequent degradation of multi-attempt performance (Pass@k) despite improvements in single-attempt accuracy (Pass@1). This is often accompanied by catastrophic forgetting, where models lose previously acquired skills. Despite numerous proposed methods, the community’s focus on the standard reverse-KL divergence has led to a surprising oversight: the potential of alternative f-divergences as a proactive solution has been largely unexamined. We argue that standard RLVR objectives—both those using the mode-seeking reverse-KL divergence and those forgoing a divergence term entirely—lack a crucial mechanism for knowledge retention. The reverse-KL actively accelerates this decay by narrowing the policy, while its absence provides no safeguard against the model drifting from its diverse knowledge base. We propose a fundamental shift in perspective: using the divergence term itself as the solution. Our framework, Diversity-Preserving Hybrid RL (DPH-RL), leverages mass-covering f-divergences (like forward-KL and JS-divergence) to function as a ‘rehearsal mechanism’. By continuously referencing the initial policy, this approach forces the model to maintain broad solution coverage. Math and SQL generation experiments show that DPH-RL both improves in-domain Pass@1 and Pass@k scores and effectively prevents catastrophic forgetting on out-of-domain tasks. Additionally, DPH-RL is more training-efficient because it computes f-divergence using generator functions, requiring only sampling from the initial policy and no online reference model. Our work highlights a crucial, overlooked axis for improving RLVR, demonstrating that the proper selection of a divergence measure is a powerful tool for building more general and diverse reasoning models.

1 INTRODUCTION

Reinforcement Learning with Verifiable Rewards (RLVR) has recently shown significant success in enhancing the mathematical and coding capabilities of Large Language Models (LLMs) (OpenAI, 2023; Team, 2024; Yang et al., 2025; Meta AI, 2024; Guo et al., 2025). Despite this progress, a critical paradox has emerged: while RLVR-tuned models consistently improve the probability of generating a correct solution in a single attempt (Pass@1), their performance when multiple attempts are permitted (Pass@k) often stagnates or even degrades compared to their base models (Yue et al., 2025). This discrepancy suggests that RLVR, rather than teaching novel reasoning, may instead overfit the model to known solution paths, thereby sacrificing diversity.

To counteract the narrowing of the model’s output distribution (Wang et al., 2025b; Yue et al., 2025), which reduces solution diversity, researchers have explored several parallel strategies. One major line of work attributes the phenomenon to entropy collapse and encourages exploration by controlling entropy (Cui et al., 2025; Cheng et al., 2025; Liang et al., 2025). Another distinct approach

*Corresponding author.

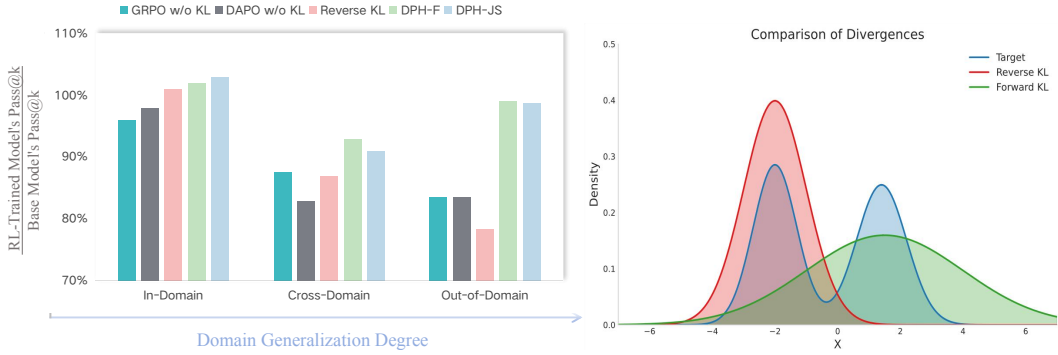
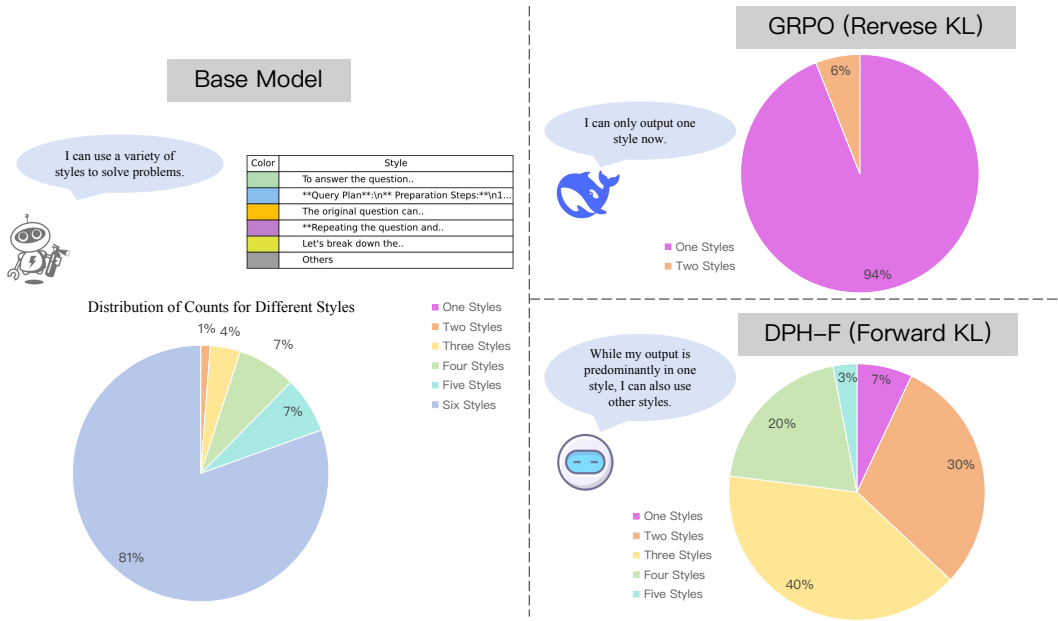


Figure 1: The left panel evaluates the performance gap in Pass@k between the RL-trained model and the Base Model across test sets with varying degrees of divergence from the training data. The right panel visualizes the distributions of reverse-KL and forward-KL.



focuses on directly optimizing the Pass@k metric (Mahdavi et al.; Walder & Karkhanis, 2025), which serves as a more direct proxy for solution diversity than entropy. A third strategy focuses on training setups, such as using extra data (Yan et al.; Dong et al., 2025a; Wang et al., 2025a), fine-tuning hyperparameters (He et al., 2025; Yu et al., 2025), or employing a hybrid RL+supervised fine-tuned (SFT) training paradigm (Liu et al., 2025b). Alongside these methods, a fourth, more fundamental component of the RL objective—the Kullback-Leibler (KL) divergence term used to constrain policy updates—also plays a crucial role.

However, while the first three avenues have been extensively explored, the influence of the KL divergence term has remained largely under-examined. The community has almost universally adopted the standard **reverse-KL divergence** ($D_{KL}(\pi_\theta || \pi_{ref}) = \mathbb{E}_{\pi_\theta} \log \frac{\pi_\theta}{\pi_{ref}}$) (Kazemnejad et al., 2024; Schulman et al., 2017; Shao et al., 2024), whose well-established **mode-seeking** nature (Bishop & Nasrabadi, 2006; Deng et al., 2025b) theoretically forces the policy to converge on a single high-probability solution. Our experiments confirm this: a reverse-KL objective yields a single solution style, while a forward-KL objective generates multiple styles (Figure 2). Additionally, we observe

that models trained with a reverse-KL term or *no KL* term at all suffer from a decline in Pass@k and catastrophic forgetting. As shown in the left panel of Figure 1, both GRPO without KL (Shao et al., 2024), DAPO (Yu et al., 2025), and Reverse KL show a significant decline in Pass@k performance. In out-of-domain scenarios, the Reverse KL approach performs even worse. These models only correctly answer about 85% of the problems they were previously able to solve (Figure 4). This phenomenon is a known challenge in sequential learning paradigms with neural networks, not a fundamental flaw of RL, which in principle does not suffer from this in tabular cases (Hamadanian et al., 2025).

Despite these significant issues, prior RLVR methods have almost exclusively relied on the standard **reverse-KL divergence**, while the exploration of other f-divergences has been largely confined to offline RL or alignment tasks (“f-PO” and “f-DPO”) (Wang et al.; Han et al., 2025b). This trend severely underestimates their potential to solve the diversity collapse problem. To bridge this critical gap, we introduce the Diversity-Preserving Framework (DPH-RL), an approach that employs different f-divergences to preserve model diversity within the online RLVR framework. A straightforward example is the **forward-KL divergence** ($D_{KL}(\pi_{ref} || \pi_\theta) = \mathbb{E}_{\pi_{ref}} \log \frac{\pi_{ref}}{\pi_\theta}$), whose theoretical **mass-covering** property penalizes the policy for failing to cover all solutions in the reference distribution. From a practitioner’s standpoint, the forward-KL objective effectively creates an “anchor dataset”, forcing the model to continuously rehearse its original knowledge base—a mechanism that mirrors human learning and prevents the catastrophic forgetting seen with reverse-KL. We generalize this concept to the broader family of **f-divergences**, including Jensen-Shannon (JS) divergence and α -divergence. Our experiments demonstrate that these mass-covering divergences, specifically forward-KL and JS-divergence, lead to significant improvements in both Pass@1 and Pass@k, maintain strong out-of-domain performance, and achieve these gains without external models. Notably, this approach is **orthogonal** to existing methods that focus on entropy control or reward shaping.

We make three main contributions:

1. Systematic Analysis of Diversity Collapse: Focusing on the KL divergence term, we provide a systematic analysis of the solution diversity collapse in RLVR, identifying the standard reverse-KL divergence as a primary cause. We show that its mode-seeking nature not only suppresses Pass@k performance—often to levels below the base model—but also exacerbates catastrophic forgetting and leads to poor out-of-domain generalization.
2. A Novel DPH-RL Framework: We reframe the role of the KL divergence, proposing its use not as a mere policy constraint but as an active diversity-preserving mechanism. Based on this principle, we introduce DPH-RL, a novel framework that employs mass-covering f-divergences (e.g., Forward-KL and JS-divergence) to serve as a rehearsal mechanism, effectively improving both Pass@1 and Pass@k performance.
3. Extensive Empirical Validation: Through extensive experiments on a range of models (Llama and Qwen, 7B to 32B) and complex reasoning tasks (mathematics and SQL), we demonstrate the robustness and superiority of DPH-RL. Our method consistently outperforms prior work on both in-domain and out-of-domain benchmarks, successfully mitigating the trade-off between greedy performance and solution diversity.

2 RELATED WORK

A more recent development is RLVR (Yue et al., 2025), a promising strategy for boosting LLM reasoning, especially in areas like mathematics, coding and reasoning (Shao et al., 2024; Team, 2024; Lambert et al., 2025; Li et al., 2024c; Han et al., 2025a). The first model to use RL to effectively encourage large-scale reasoning was OpenAI’s o1 (OpenAI, 2024). Following its success, models like DeepSeek R1 (Guo et al., 2025), QwQ (Qwen, 2024), Kimi k1.5 (Team et al., 2025), and Qwen3 (Yang et al., 2025) have been developed with the goal of matching or exceeding its performance. Notably, DeepSeek R1 demonstrated that robust reasoning can arise from optimizing based on outcomes using the GRPO online RL algorithm (Shao et al., 2024). A significant challenge that has received attention is policy diversity collapse in RLVR. To address this, one major line of research focuses on either directly controlling model entropy (Cui et al., 2025; Prabhudesai et al., 2025; Agarwal et al., 2025; Li et al., 2025; Cheng et al., 2025; Liang et al., 2025) or strategically capturing high-entropy tokens (Wang et al., 2025b; Chen et al., 2025a; MiniMax et al., 2025). However, some research suggests that the entropy of specific tokens is more strongly correlated with model diversity than sentence-level entropy (Wang et al., 2025b; Cheng et al., 2025; Deng et al.,

2025a; Chen et al., 2025a); consequently, other methods maintain training diversity by controlling the model’s Pass@k metric (Chen et al., 2025b; Dong et al., 2025b). From a training design perspective, methods such as dynamically adjusting rollout-related hyperparameters (An et al., 2025; He et al., 2025; Yu et al., 2025) or using a hybrid SFT+RL (Liu et al., 2025b; Lv et al., 2025; Liu et al., 2025a;c) training paradigm are also employed to prevent diversity collapse.

Our work is most closely related to recent studies that explore f-divergences for policy optimization. Notably, Wang et al. (2024); Han et al. (2025b) **replace the reverse-KL divergence in the offline DPO objective with a generalized f-divergence, deriving a new family of “f-PO” algorithms. However, our work is distinct in both its objective and methodology.** The f-PO methods operate in an offline setting using human preference data to improve alignment. In contrast, our work operates in an online RLVR setting, using verifiable rewards from reasoning tasks. Our primary goal is not preference alignment, but specifically to solve the Pass@k diversity collapse by leveraging the properties of mass-covering f-divergences.

3 PRELIMINARIES

3.1 f -DIVERGENCE

In information theory, an *f*-divergence is a function $D_f(p\|q)$ that measures the difference between two probability distributions p and q . Given a convex function $f : \mathbb{R}^+ \rightarrow \mathbb{R}$ such that $f(1) = 0$, the f-divergence is defined as:

$$D_f(p\|q) = \int q(x)f\left(\frac{p(x)}{q(x)}\right)dx$$

This general form allows for the unification of many common divergence measures under a single theoretical framework. The condition $f(1) = 0$ ensures that $D_f(p\|q) = 0$ if and only if $p = q$. Many common divergences are special cases of f-divergences, corresponding to a specific choice for the generator function f . For instance, KL divergence and JS divergence are all instances of f-divergences. The generator function for JS divergence is $(u \log u - (u+1) \log \frac{u+1}{2})/2$. A summary of some prominent f-divergences and their corresponding generator functions is provided in Table 5.

3.2 MARKOV DECISION PROCESS

We consider a discounted Markov Decision Process (MDP) defined by the tuple $(\mathcal{S}, \mathcal{A}, P, r, \rho_0, \gamma)$, where \mathcal{S} is the state space, \mathcal{A} is the action space, $P(s'|s, a)$ is the transition probability, $r(s)$ is the reward function, ρ_0 is the initial state distribution, and $\gamma \in [0, 1)$ is the discount factor. A stochastic policy $\pi(a|s)$ defines a probability distribution over actions for each state. The goal is to maximize the performance objective, i.e., the expected cumulative discounted reward:

$$J(\pi) = \mathbb{E}_{\tau \sim \pi} \left[\sum_{t=0}^{\infty} \gamma^t r(s_t) \right], \quad \text{where } s_0 \sim \rho_0(s_0), a_t \sim \pi(a_t|s_t), s_{t+1} \sim P(s_{t+1}|s_t, a_t). \quad (1)$$

A seminal result from Kakade & Langford (2002) expresses the performance of a policy π in terms of an older policy π_{old} using the advantage function $A_{\pi_{\text{old}}}(s, a)$: $J(\pi) = J(\pi_{\text{old}}) + \mathbb{E}_{\tau \sim \pi} [\sum_{t=0}^{\infty} \gamma^t A_{\pi_{\text{old}}}(s_t, a_t)]$. This can be rewritten using the discounted state visitation distribution, $\rho_{\pi}(s) \triangleq \sum_{t=0}^{\infty} \gamma^t P(s_t = s | \pi)$, which gives the probability distribution over states encountered under policy π :

$$J(\pi) = J(\pi_{\text{old}}) + \sum_{s \in \mathcal{S}} \rho_{\pi}(s) \sum_{a \in \mathcal{A}} \pi(a|s) A_{\pi_{\text{old}}}(s, a). \quad (2)$$

Directly optimizing this expression is difficult because the state distribution ρ_{π} depends on the new policy π . Therefore, algorithms like TRPO and PPO optimize a surrogate objective $L_{\pi_{\text{old}}}(\pi)$ by approximating ρ_{π} with the distribution from the old policy, $\rho_{\pi_{\text{old}}}$:

$$L_{\pi_{\text{old}}}(\pi) = J(\pi_{\text{old}}) + \sum_{s \in \mathcal{S}} \rho_{\pi_{\text{old}}}(s) \sum_{a \in \mathcal{A}} \pi(a|s) A_{\pi_{\text{old}}}(s, a). \quad (3)$$

This approximation is reliable when π is close to π_{old} , forming the basis of modern policy gradient methods.

4 METHOD

In this section, we detail our implementation of reinforcement learning (RL) with an f-divergence regularizer. Our objective is to find the optimal policy for the following optimization problem:

$$\max_{\pi_\theta} \mathbb{E}_{q \sim \mathcal{D}} [\mathbb{E}_{a \sim \pi_\theta(\cdot|q)} [r(a|q)] - \eta D_f(\pi_\theta(\cdot|q) || \pi_{ref}(\cdot|q))]. \quad (4)$$

In this formulation, π_{ref} serves as the initial reference policy, such as a base or SFT model. The term $r(a|q)$ represents the reward for taking action a in response to query q , and the hyperparameter η controls the penalty for deviating from π_{ref} . While standard algorithms like PPO can optimize the reward term, our discussion focuses on estimating the f-divergence term. A uniform application of this approach across all queries in dataset \mathcal{D} can be suboptimal. For queries where π_{ref} performs well, aggressive reward maximization is unnecessary and risks degrading performance. Conversely, for challenging queries where π_{ref} struggles, the f-divergence term can overly constrain the policy π_θ , limiting its ability to explore better solutions. To address this, we propose a targeted strategy that partitions the dataset \mathcal{D} into two subsets. The methodology is divided into two phases: a **pre-sampling stage** and an **online training stage**.

4.1 PRE-SAMPLING STAGE

We consider a specific instance of f-divergence, **Forward-KL**, defined as:

$$D_{\text{forward-KL}}(\pi_\theta || \pi_{ref}) \triangleq D_{\text{KL}}(\pi_{ref} || \pi_\theta) = \mathbb{E}_{a \sim \pi_{ref}} [\log(\pi_{ref}(a|q)) - \log(\pi_\theta(a|q))].$$

To facilitate computing this expectation, we adopt a pre-sampling strategy. Before training π_θ , we partition the dataset \mathcal{D} . For each query Q , we generate and evaluate k independent samples. Based on a correctness threshold, each query is classified as either “**near-perfect**” or “**exploration**,” splitting \mathcal{D} into \mathcal{D}_{pef} and \mathcal{D}_{exp} . This partition allows our agent to focus on challenging examples in \mathcal{D}_{exp} while using a KL divergence constraint to maintain performance on mastered examples in \mathcal{D}_{pef} . To mitigate sampling bias, we further refine \mathcal{D}_{pef} . For each query in this subset, we draw one final sample. We only retain the query in \mathcal{D}_{pef} if this new sample is correct; otherwise, we discard the query or move it to \mathcal{D}_{exp} .

4.2 ONLINE TRAINING STAGE

In the online training stage, we simultaneously train the model using two distinct loss functions tailored for the \mathcal{D}_{exp} and \mathcal{D}_{pef} datasets. For samples from \mathcal{D}_{exp} , we want the model to have maximum freedom for exploration. Conversely, for samples from \mathcal{D}_{pef} , we want the model to retain its capabilities. To achieve this, we employ two key f-divergences: **Forward-KL** and **JS divergence**. Our method is thus divided into two approaches: **DPH-F** for forward-KL and **DPH-JS** for JS divergence. Forward-KL divergence, as we define it, penalizes instances where the reference policy π_{ref} assigns a high probability to an action, but the new policy π_θ assigns a near-zero probability. This property encourages the new policy π_θ to maintain coverage of all modes of the reference policy π_{ref} , thereby preserving its original diversity. JS divergence provides a symmetric and more stable alternative to KL divergence. It encourages the new policy π_θ to maintain high similarity with the reference policy π_{ref} while achieving high performance, effectively preventing policy collapse.

4.2.1 GENERATOR-BASED IMPLEMENTATION

Our implementation relies on pre-sampling from the reference policy. This approach allows us to compute the divergence term using a static dataset, eliminating the need to run inference with the reference model during the online training loop.

Loss for \mathcal{D}_{exp} For challenging samples in \mathcal{D}_{exp} , we remove the KL divergence penalty from the loss function entirely. This allows the model to perform pure policy optimization based solely on the reward signal, enabling more aggressive exploration. Specifically, the loss function for these samples is the standard PPO-clip objective:

$$\mathcal{L}_{\text{DPH-exp}}(\theta) = -\mathbb{E}_{\substack{q \sim \mathcal{D}_{\text{exp}} \\ o_i \sim \pi_{\theta_{\text{old}}}(\cdot|q)}} \left[\frac{1}{G} \sum_{i=1}^G \frac{1}{|o_i|} \sum_{t=1}^{|o_i|} \min \left(\rho_{i,t}(\theta) \hat{A}_{i,t}, \right. \right. \\ \left. \left. \text{clip}(\rho_{i,t}(\theta), 1 - \varepsilon, 1 + \varepsilon) \hat{A}_{i,t} \right) \right] \quad (5)$$

Please refer to Appendix D for the definitions of the symbols in the formula.

Loss for \mathcal{D}_{pef} For all f-divergences, the general formula for calculating the loss on \mathcal{D}_{pef} is:

$$\mathcal{L}_{\text{pef}}(\theta) = \mathbb{E}_{q \sim \mathcal{D}_{\text{pef}}} [D_f(\pi_{\theta} || \pi_{\text{ref}})]. \quad (6)$$

For DPH-F, the loss term is: $\mathbb{E}_{q \sim \mathcal{D}_{\text{pef}}} \left[\sum_a \pi_{\text{ref}}(a|q) \log \left(\frac{\pi_{\text{ref}}(a|q)}{\pi_{\theta}(a|q)} \right) \right]$, where a represents a single response sampled once from the reference policy $\pi_{\text{ref}}(\cdot|q)$. For DPH-JS, the loss term is: $\mathbb{E}_{q \sim \mathcal{D}_{\text{pef}}} \left[\sum_a \pi_{\text{ref}}(a|q) \left(\frac{u \log u}{2} - \frac{u+1}{2} \log \left(\frac{u+1}{2} \right) \right) \right]$, where $u = \pi_{\theta}(a|q)/\pi_{\text{ref}}(a|q)$.

4.2.2 OVERALL LOSS FUNCTION

The total loss for a given batch is a combination of these two objectives. For a mixed batch, we determine whether the data comes from \mathcal{D}_{pef} or \mathcal{D}_{exp} and then calculate the corresponding loss:

$$\mathcal{L}_{\text{DPH-RL}}(\theta) = \mathcal{L}_{\text{exp}}(\theta) + \eta \mathcal{L}_{\text{pef}}(\theta), \quad (7)$$

4.3 ENHANCED MONOTONIC IMPROVEMENT GUARANTEE

In this section, we derive an enhanced monotonic improvement guarantee for TRPO-style algorithms that leverage our proposed method. Our framework is built upon two distinct datasets: \mathcal{D}_{pef} , which stores near-perfect reasoning trajectories, and \mathcal{D}_{exp} , an exploration set for tasks the model has not yet mastered. Central to our analysis is a conditional reference policy, π_{pef} , whose definition depends on the data source. For states associated with the **near-perfect dataset** (\mathcal{D}_{pef}), π_{pef} is the policy induced by the stored correct trajectories. The f-divergence regularization term $D_f(\pi || \pi_{\text{pef}})$ pulls the learned policy π towards these expert solutions. For states associated with the **exploration dataset** (\mathcal{D}_{exp}), π_{pef} is defined as the current policy π . This makes the regularization term $D_f(\pi || \pi)$ equal to zero, thereby disabling it and permitting unrestricted exploration. To analyze the effect of this conditional regularization, our derivation hinges on the following mild assumption.

Assumption 1. *For any policy π encountered during training, there exists a constant $\delta \geq 0$ such that for any state s , the expected advantage of actions from the reference policy π_{pef} , evaluated with respect to π , is lower-bounded by δ : $\mathbb{E}_{a_{\text{pef}} \sim \pi_{\text{pef}}(\cdot|s)} [A^{\pi}(s, a_{\text{pef}})] \geq \delta$.*

This assumption is well-founded. In regions of the state space well-represented by the near-perfect dataset \mathcal{D}_{pef} , the actions from π_{pef} are expected to be superior, yielding a positive advantage ($\delta > 0$). Conversely, for states associated with \mathcal{D}_{exp} , where our method effectively applies no regularization, the bound trivially holds with $\delta = 0$. Leveraging this assumption, we present the following theorem, which establishes a stronger lower bound on policy improvement than the one in the original TRPO analysis (Schulman et al., 2015).

Theorem 1 (Enhanced Monotonic Improvement). *Let $\alpha_1 = \max_s D_{\text{KL}}(\pi(\cdot|s) || \pi_{\text{old}}(\cdot|s))$ and $\alpha_2 = \max_s D_f(\pi(\cdot|s) || \pi_{\text{pef}}(\cdot|s))$, where the divergence D_f can be the forward-KL, α -divergence, or Jensen-Shannon divergence. If Assumption 1 holds, then the following bound on policy improvement is guaranteed:*

$$J(\pi) - L_{\pi_{\text{old}}}(\pi) \geq -\frac{2\gamma\alpha_1\epsilon_{\pi}}{(1-\gamma)^2} + \epsilon_f \quad (8)$$

where $\epsilon_f = \frac{\delta}{1-\gamma} - \frac{C_f \gamma \alpha_2 \epsilon_{\text{pef}}}{(1-\gamma)^2}$, $\epsilon_{\pi} = \max_{s,a} |A_{\pi}(s, a)|$ and $\epsilon_{\text{pef}} = \max_{s,a} |A_{\pi_{\text{pef}}}(s, a)|$, C_f is a positive constant depending on the choice of the f-divergence.

Comparing with the monotonic improvement theorem in Schulman et al. (2015), where the right hand side of the inequality is $-\frac{2\gamma\alpha_1\epsilon_f}{(1-\gamma)^2}$, we have an additional term ϵ_f . On the distribution associated with expert dataset \mathcal{D}_{pef} , where $\delta > 0$ and effective regularization keeps α_2 small, ϵ_f becomes a positive bonus. This results in a strictly better lower bound on policy improvement than in the original TRPO analysis, rigorously justifying that our method accelerates convergence by leveraging known expert behavior. On the exploration set \mathcal{D}_{exp} , the bound gracefully reduces to the standard TRPO guarantee. The proof of Theorem 1 follows a similar line of reasoning to the analyses in Schulman et al. (2015) and Kang et al. (2018). The detailed derivation is deferred to the Appendix I for the completeness.

5 EXPERIMENTS

In this section, we conduct extensive experiments to demonstrate the effectiveness and generalization of DPH-RL. The experimental setups were applied to two types of tasks: SQL (where the LLM generates SQL code and executes it using a tool) and mathematical reasoning, using both Llama 3.1 Meta AI (2024) and Qwen2.5 Team (2024) series models. In our experiments, we partition the dataset into \mathcal{D}_{exp} and \mathcal{D}_{pef} based on the capabilities of each model. For the Llama model, we define the \mathcal{D}_{pef} using a success rate of 6 out of 8 attempts, while for the Qwen model, this threshold is raised to 7 out of 8 attempts. Since our method is orthogonal to existing GRPO variants, we use GRPO, DAPO, and reverse-KL (RKL) as baselines. Please refer to Appendix F for training details.

5.1 SQL

Table 1: Results of **Llama-3.1-8B-Instruct** on SQL Tasks. The highest scores for RL Models are highlighted. Figure 6 shows the error bars for each method over three training runs.

| Model | Bird | | | Spider | | |
|---|--------|--------|---------|--------|--------|---------|
| | Greedy | Pass@8 | Pass@16 | Greedy | Pass@8 | Pass@16 |
| Base Model | 42.4 | 68.8 | 75.0 | 71.0 | 90.9 | 93.2 |
| <i>RL Models</i> | | | | | | |
| GRPO | 58.5 | 66.2 | 67.7 | 73.0 | 79.5 | 80.6 |
| DAPO | 60.0 | 67.2 | 69.0 | 71.1 | 75.3 | 76.7 |
| RKL | 60.0 | 69.8 | 71.8 | 71.0 | 79.0 | 80.6 |
| DPH-F | 60.4 | 70.1 | 71.6 | 77.4 | 84.5 | 85.7 |
| α Divergence | | | | | | |
| $-\alpha=0.2$ | 60.1 | 67.0 | 69.1 | 75.4 | 78.8 | 80.1 |
| $-\alpha=0.5$ | 60.8 | 68.0 | 69.8 | 75.2 | 80.4 | 82.5 |
| $-\alpha=0.8$ | 60.5 | 69.2 | 70.4 | 75.8 | 81.7 | 83.6 |
| DPH-JS (<i>Generator</i>) | | | | | | |
| $-\eta=0.01$ | 59.8 | 66.7 | 68.1 | 76.4 | 79.1 | 80.8 |
| $-\eta=0.05$ | 61.3 | 69.5 | 70.9 | 75.3 | 82.7 | 83.8 |
| $-\eta=0.2$ | 62.8 | 70.5 | 72.4 | 76.0 | 82.7 | 84.1 |
| DPH-JS (<i>Divergence Definition</i>) | | | | | | |
| $-\eta=0.01$ | 59.6 | 66.6 | 68.2 | 76.7 | 80.5 | 81.5 |
| $-\eta=0.05$ | 61.4 | 69.6 | 71.3 | 75.9 | 83.5 | 84.7 |
| $-\eta=0.2$ | 62.4 | 70.1 | 71.9 | 78.6 | 85.2 | 86.7 |

As shown in Table 1, in the Bird dataset, the Pass@8 scores for both GRPO and DAPO are lower than the base model, while our DPH-F and DPH-JS methods surpass the base model. This indicates that our strategy possesses a more robust ability to maintain model diversity. Specifically, DPH-JS shows Pass@8 scores that are 4.3% and 3.3% higher than GRPO and DAPO, respectively. For the Spider dataset, which is a cross-domain SQL task, the Pass@k metrics for all models generally suffer from performance degradation. However, DPH-F and DPH-JS can maintain accuracy levels closer to the base model. While DAPO performs better than GRPO on the Bird dataset, its performance is more unstable on the cross-domain data. Regarding cross-domain performance

Table 2: Results on Omnisql-32B for SQL tasks. * Indicates that the results are from the Bird Bench.

| Model | Bird | | | Spider | | |
|-------------------------|--------|--------|---------|--------|--------|---------|
| | Greedy | Pass@8 | Pass@16 | Greedy | Pass@8 | Pass@16 |
| OmnisQL-32B | | | | | | |
| Base Model | 65.0 | 77.3 | 79.8 | 85.0 | 92.8 | 93.6 |
| <i>Other Models</i> | | | | | | |
| Infly-RL-SQL-32B* | 70.1 | - | - | - | - | - |
| XiYanSQL-QwenCoder-32B* | 67.0 | - | - | - | - | - |
| Arctic-ExCoT-70B* | 68.5 | | | | | |
| Command A* | 63.5 | | | | | |
| <i>RL Models</i> | | | | | | |
| GRPO | 69.4 | 76.3 | 78.8 | 84.7 | 91.6 | 92.4 |
| DAPO | 69.9 | 76.8 | 79.2 | 83.8 | 91.0 | 91.7 |
| DPH-F | 70.4 | 78.6 | 80.8 | 86.1 | 92.7 | 93.3 |
| DPH-JS | 70.5 | 79.2 | 81.9 | 84.9 | 91.9 | 93.1 |

Table 3: Out-of-Domain Performance. Evaluating SQL-trained models on mathematical tasks.

| Model | Pass@64 | | Pass@16 | | | Pass@8 | | Avg |
|--|---------|-------|---------|----------|---------|--------------|-------|-----|
| | AIME24 | AMC23 | Math500 | Olympiad | Minerva | College Math | | |
| Llama-3.1-8B-Instruct (SQL-trained) | | | | | | | | |
| Base Model | 40.0 | 95.0 | 81.2 | 46.4 | 54.0 | 45.5 | 60.35 | |
| <i>RL Models</i> | | | | | | | | |
| -GRPO | 33.3 | 77.5 | 72.0 | 41.8 | 51.2 | 38.4 | 52.37 | |
| -DAPO | 30.0 | 77.5 | 72.8 | 44.4 | 52.3 | 38.8 | 52.63 | |
| -RKL | 23.3 | 72.5 | 70.8 | 33.8 | 49.2 | 41.1 | 48.45 | |
| $-\alpha=0.2$ | 40.0 | 90.0 | 79.8 | 44.0 | 51.8 | 41.8 | 57.90 | |
| $-\alpha=0.5$ | 36.7 | 85.0 | 80.2 | 43.7 | 50.7 | 43.4 | 56.62 | |
| $-\alpha=0.8$ | 43.3 | 87.5 | 80.8 | 43.1 | 54.0 | 44.2 | 58.82 | |
| DPH-F | 46.7 | 95.0 | 80.8 | 46.1 | 54.3 | 43.0 | 60.98 | |
| DPH-JS | 40.0 | 92.5 | 81.2 | 48.2 | 53.8 | 45.7 | 60.23 | |

preservation, DPH-F demonstrates a more powerful capability, with its Pass@16 scores being 9.0% higher than DAPO. This suggests that for simple tasks that the model can already handle correctly, preservation of its original capabilities is more crucial than pure exploration. We conducted experiments on **OmnisQL-32B**, with the results presented in Table 2. Its Greedy performance on the Bird dataset surpasses all current open-source models.

Ablation Study Our method introduces a plug-and-play f -divergence loss, weighted by a hyperparameter η , which we analyze in an ablation study. As shown in Table 1, when the value of η is minimal, its actual setup and performance approximate that of DAPO trained exclusively on \mathcal{D}_{ref} . Increasing the value of η leads to steady growth in the Pass@16 score, demonstrating the effectiveness of our method. Additionally, we compared two implementations of f -divergence: the “Generator” form and the “Divergence Definition” form (detailed in Appendix E). Although both yield similar performance, the “Divergence Definition” form is computationally expensive as it requires resampling from π_θ and an additional reference model to calculate $\pi_{\text{ref}}(a|q)$. Consequently, the “Generator” form is significantly more time-efficient.

Performance on OOD Tasks As shown in Table 3, we evaluated the diversity of our RL-trained models on five out-of-domain (OOD) mathematical datasets using a Llama model. (We excluded the AIME25 dataset due to its high fluctuation, ensuring a fair comparison.) Without incorporating additional general-purpose data, methods like GRPO and DAPO cause models to overfit to the SQL training domain, leading to a significant drop in performance on other OOD tasks. In contrast, our DPH-F and DPH-JS methods maintain a higher average performance, surpassing DAPO by 8.35% and 7.6%, respectively.

Comparisons Under Different f -divergences In Tables 1 and 3, we analyzed the impact of different f -divergences on the Llama model. First, DAPO and GRPO, which lack any form of f -divergence constraint, experienced severe Pass@k collapse on both in-domain and out-of-domain tasks. Conversely, while RKL could maintain a high Pass@k on the training task’s test set, its performance collapse on tasks with different distributions was even more severe than methods without any KL penalty. This highlights the limitations of reverse-KL: it causes the model to over-focus on the training data’s distribution, thereby completely sacrificing generalization. To validate the reliability of our experimental baseline, we show the performance of RKL with different η values in Figure 3. When $\eta > 0.02$, the model’s learning performance fails to surpass that of DAPO. This indicates that the chosen η value is too large, and therefore our selection of $\eta = 0.01$ is well-justified.

The α divergence sits between the forward-KL and reverse-KL, effectively preventing the model from veering toward extremes. Across all datasets, it shows a clear trend: as the α value increases, it theoretically approaches the capabilities of forward-KL, while experimentally maintaining a higher Pass@k. In contrast, DPH-F and DPH-JS methods demonstrated strong generalization across different tasks. The DPH-JS method, in particular, not only maintained a higher greedy performance on training tasks but also preserved a high Pass@k value on out-of-domain tasks, which fully demonstrates its significant advantage in preserving a multi-peak distribution.

5.2 MATHEMATICAL REASONING

Table 4: The Pass@k metric for models trained on math datasets. In the Llama experiments, the DAPO settings ($\epsilon_{\text{high}}=0.28$) caused training to crash. To conduct effective experiments, we aligned the settings for all Llama experiments on the Math dataset with GRPO ($\epsilon_{\text{high}}=0.2$).

| Model | Pass@64 | | | Pass@16 | | | Pass@8 | | Avg |
|------------------------------|---------|--------|-------|---------|----------|---------|--------------|-------|-----|
| | AIME24 | AIME25 | AMC23 | Math500 | Olympiad | Minerva | College Math | | |
| Llama-3.1-8B-Instruct | | | | | | | | | |
| Base Model | 40.0 | 23.3 | 95.0 | 81.2 | 46.4 | 54.0 | 45.5 | 55.06 | |
| RL Models | | | | | | | | | |
| -GRPO | 33.3 | 26.7 | 80.0 | 79.6 | 43.3 | 56.6 | 43.1 | 51.80 | |
| -RKL | 36.7 | 16.7 | 75.0 | 80.0 | 39.1 | 56.6 | 43.4 | 49.64 | |
| -DPH-F | 36.7 | 26.7 | 90.0 | 80.6 | 44.3 | 57.3 | 45.5 | 54.44 | |
| -DPH-JS | 40.0 | 26.7 | 82.5 | 81.4 | 45.8 | 58.1 | 45.1 | 54.23 | |
| Qwen2.5-Math-7B | | | | | | | | | |
| Base Model | 63.3 | 56.7 | 87.5 | 88.8 | 61.9 | 56.6 | 42.9 | 65.39 | |
| RL Models | | | | | | | | | |
| -GRPO | 56.6 | 50.0 | 97.5 | 93.0 | 62.8 | 64.0 | 50.1 | 67.71 | |
| -DAPO | 63.3 | 46.7 | 97.5 | 92.2 | 63.1 | 64.3 | 48.7 | 67.97 | |
| -RKL | 66.7 | 40.0 | 97.5 | 92.0 | 64.6 | 64.0 | 51.3 | 68.01 | |
| -DPH-F | 73.33 | 50.0 | 97.5 | 92.4 | 63.8 | 64.8 | 50.9 | 70.39 | |
| -DPH-JS | 66.7 | 53.3 | 100.0 | 92.8 | 65.2 | 66.2 | 51.0 | 70.74 | |

For the mathematical tasks, we present two types of results, shown in Table 4 and Table 8, respectively. Table 4 shows the Pass@k scores on various test sets, while Table 8 shows the Mean@k scores, which is the average accuracy calculated by sampling the entire dataset k times. Regarding mathematical ability, different model families have completely different capabilities. For the Llama model, the improvement through RL is very limited; the average mean@k value when using GRPO only increased by 0.93, while Pass@k decreased by 3.26. By contrast, the Qwen model is a more capable model, which allows it to achieve a significant boost in both Mean@k (approximately 20%) and Pass@k.

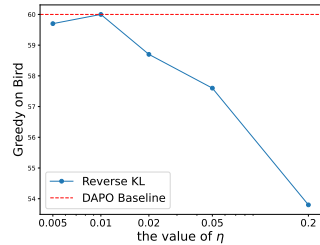


Figure 3: η vs. Greedy

When $\eta > 0.02$, the model’s

We selected these two models to explore the performance of the DPH method under different model strengths. For Llama, DPH-JS maintained the original Pass@k value and significantly improved mean@k on AIME, which demonstrates that DPH-JS is a powerful and highly versatile method with strong capabilities in both exploration and preservation. Furthermore, DPH-JS provided a more balanced improvement than GRPO, increasing both Pass@k and mean@k averages, showing it does not sacrifice one metric for the other. For the Qwen model, the overall performance showed a dual trend: a slight decrease in Pass@k on the difficult AIME test set, but an increase on other, simpler datasets. In both scenarios, the DPH-JS method achieved the best performance. On AIME, it maintained a diversity closer to that of the base model compared to both GRPO and DAPO. On the other datasets, it achieved a higher Pass@k. This trend highlights a key challenge for large models in RL: the need to both solidify existing knowledge while also exploring new boundaries. The DPH-JS method successfully balances these two conflicting goals.

6 ANALYSIS OF KEEP AND EXPLORATION

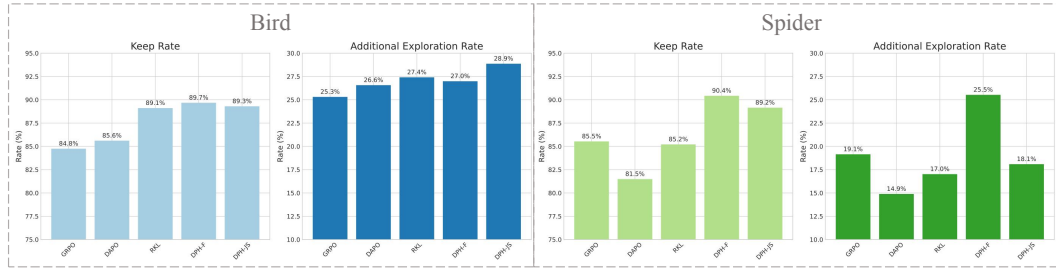


Figure 4: Exploring the differences between base model and RL-Tuned models in Llama.

To gain a more granular understanding of why our method achieves higher Pass@k scores, we extracted correct and incorrect samples from the base model’s Pass@8 results. These were designated as data subsets $D_{sub}^{correct}$ and D_{sub}^{wrong} , respectively. We then compared them with the model after reinforcement learning. The proportion of samples it got correct on $D_{sub}^{correct}$ is its keep rate, while the proportion it got correct on the incorrect samples from D_{sub}^{wrong} is its additional exploration rate. As shown in Figure 4, the keep rate of GRPO and DAPO both decreased on the two datasets, while the KL method mainly maintained a higher keep rate to maintain a higher Pass@k value. DAPO had higher exploration within the domain than GRPO, but the keep rate outside the domain dropped significantly. RKL could only have a high keep rate on the same Bird test set as the training set, while it dropped to a level similar to GRPO on Spider. DPH-JS had higher exploration on the Bird test set, while DPH-F was higher on the Spider dataset.

6.1 ANALYSIS OF TRAINING PROGRESS

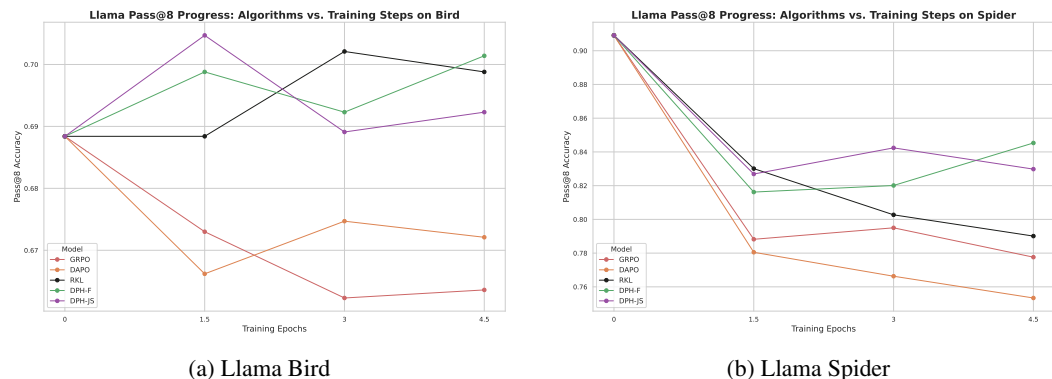


Figure 5: Llama Pass@8 progress: Algorithms vs. Training Steps

In Figure 5, we visualize the evolution of the Llama model’s Pass@8 metric during training. On the Bird dataset, GRPO shows a clear, gradual collapse, while DAPO’s performance continuously oscillates. Over the long term, DPH-F and DPH-JS both consistently maintain a higher Pass@8 value than the initial level. On the Spider dataset, DAPO performs extremely poorly, even falling below GRPO. Our experiments show that DAPO sacrifices out-of-domain generalization for improved performance on in-domain datasets. While RKL performs well on the Bird dataset, its performance also shows a gradual collapse on the Spider dataset as training progresses.

7 CONCLUSION

We propose DPH-RL to overcome the limitations of reverse KL divergence in reinforcement learning for LLMs. By leveraging f -divergence, our method mitigates both diversity collapse and catastrophic forgetting. We demonstrate that two implementations—a “Generator” form that requires no reference model during training and a “Divergence Definition” form—yield similar performance. This makes our method highly adaptable, providing enhanced capabilities with computational costs comparable to GRPO. However, a key limitation, shared with GRPO, is the dependence on the base model’s capabilities, which become scarce on more challenging datasets. Future work will therefore focus on resolving this trade-off, aiming to develop methods that can both learn effectively from imperfect data and mitigate the resulting estimation bias.

REPRODUCIBILITY

Our datasets are all based on open-source datasets. The experimental methodology, data proportions, and hyperparameter settings are detailed in Appendix F.

REFERENCES

Shivam Agarwal, Zimin Zhang, Lifan Yuan, Jiawei Han, and Hao Peng. The unreasonable effectiveness of entropy minimization in llm reasoning, 2025. URL <https://arxiv.org/abs/2505.15134>.

Chenxin An, Zhihui Xie, Xiaonan Li, Lei Li, Jun Zhang, Shansan Gong, Ming Zhong, Jingjing Xu, Xipeng Qiu, Mingxuan Wang, and Lingpeng Kong. Polaris: A post-training recipe for scaling reinforcement learning on advanced reasoning models, 2025. URL <https://hkunlp.github.io/blog/2025/Polaris>.

Christopher M Bishop and Nasser M Nasrabadi. *Pattern recognition and machine learning*, volume 4. Springer, 2006.

Minghan Chen, Guikun Chen, Wenguan Wang, and Yi Yang. Seed-grpo: Semantic entropy enhanced grpo for uncertainty-aware policy optimization, 2025a. URL <https://arxiv.org/abs/2505.12346>.

Zhipeng Chen, Xiaobo Qin, Youbin Wu, Yue Ling, Qinghao Ye, Wayne Xin Zhao, and Guang Shi. Pass@k training for adaptively balancing exploration and exploitation of large reasoning models, 2025b. URL <https://arxiv.org/abs/2508.10751>.

Daixuan Cheng, Shaohan Huang, Xuekai Zhu, Bo Dai, Wayne Xin Zhao, Zhenliang Zhang, and Furu Wei. Reasoning with exploration: An entropy perspective on reinforcement learning for llms, 2025. URL <https://arxiv.org/abs/2506.14758>.

Ganqu Cui, Yuchen Zhang, Jiacheng Chen, Lifan Yuan, Zhi Wang, Yuxin Zuo, Haozhan Li, Yuchen Fan, Huayu Chen, Weize Chen, Zhiyuan Liu, Hao Peng, Lei Bai, Wanli Ouyang, Yu Cheng, Bowen Zhou, and Ning Ding. The entropy mechanism of reinforcement learning for reasoning language models, 2025. URL <https://arxiv.org/abs/2505.22617>.

Jia Deng, Jie Chen, Zhipeng Chen, Wayne Xin Zhao, and Ji-Rong Wen. Decomposing the entropy-performance exchange: The missing keys to unlocking effective reinforcement learning, 2025a. URL <https://arxiv.org/abs/2508.02260>.

Wenhao Deng, Long Wei, Changlei Yu, and Tailin Wu. Unlocking reasoning capabilities in llms via reinforcement learning exploration. *arXiv preprint arXiv:2510.03865*, 2025b.

Yihong Dong, Xue Jiang, Yongding Tao, Huanyu Liu, Kechi Zhang, Lili Mou, Rongyu Cao, Ying-wei Ma, Jue Chen, Binhu Li, et al. RL-plus: Countering capability boundary collapse of llms in reinforcement learning with hybrid-policy optimization. *arXiv preprint arXiv:2508.00222*, 2025a.

Yihong Dong, Xue Jiang, Yongding Tao, Huanyu Liu, Kechi Zhang, Lili Mou, Rongyu Cao, Ying-wei Ma, Jue Chen, Binhu Li, et al. RL-plus: Countering capability boundary collapse of llms in reinforcement learning with hybrid-policy optimization. *arXiv preprint arXiv:2508.00222*, 2025b.

Alexei A Fedotov, Peter Harremoës, and Flemming Topsøe. Refinements of pinsker's inequality. *IEEE Transactions on Information Theory*, 49(6):1491–1498, 2003.

Daya Guo, Dejian Yang, Haowei Zhang, Junxiao Song, Ruoyu Zhang, Runxin Xu, Qihao Zhu, Shirong Ma, Peiyi Wang, Xiao Bi, et al. Deepseek-r1: Incentivizing reasoning capability in llms via reinforcement learning. *arXiv preprint arXiv:2501.12948*, 2025.

Pouya Hamadanian, Arash Nasr-Esfahany, Malte Schwarzkopf, Siddartha Sen, and Mohammad Alizadeh. Online reinforcement learning in non-stationary context-driven environments. In *International Conference on Learning Representations*, 2025.

Feijiang Han, Xiaodong Yu, Jianheng Tang, Delip Rao, Weihua Du, and Lyle Ungar. Zerotuning: Unlocking the initial token's power to enhance large language models without training. *arXiv preprint arXiv:2505.11739*, 2025a.

Jiaqi Han, Mingjian Jiang, Yuxuan Song, Stefano Ermon, and Minkai Xu. f -po: Generalizing preference optimization with f -divergence minimization. In *International Conference on Artificial Intelligence and Statistics*, pp. 1144–1152. PMLR, 2025b.

Chaoqun He, Renjie Luo, Yuzhuo Bai, Shengding Hu, Zhen Leng Thai, Junhao Shen, Jinyi Hu, Xu Han, Yujie Huang, Yuxiang Zhang, Jie Liu, Lei Qi, Zhiyuan Liu, and Maosong Sun. Olympiadbench: A challenging benchmark for promoting AGI with olympiad-level bilingual multimodal scientific problems. In *ACL (1)*, pp. 3828–3850. Association for Computational Linguistics, 2024.

Jujie He, Jiacai Liu, Chris Yuhao Liu, Rui Yan, Chaojie Wang, Peng Cheng, Xiaoyu Zhang, Fuxiang Zhang, Jiacheng Xu, Wei Shen, Siyuan Li, Liang Zeng, Tianwen Wei, Cheng Cheng, Bo An, Yang Liu, and Yahui Zhou. Skywork open reasoner 1 technical report, 2025. URL <https://arxiv.org/abs/2505.22312>.

Dan Hendrycks, Collin Burns, Saurav Kadavath, Akul Arora, Steven Basart, Eric Tang, Dawn Song, and Jacob Steinhardt. Measuring mathematical problem solving with the MATH dataset. In *NeurIPS Datasets and Benchmarks*, 2021.

Sham Kakade and John Langford. Approximately optimal approximate reinforcement learning. In *Proceedings of the nineteenth international conference on machine learning*, pp. 267–274, 2002.

Bingyi Kang, Zequn Jie, and Jiashi Feng. Policy optimization with demonstrations. In *International conference on machine learning*, pp. 2469–2478. PMLR, 2018.

Amirhossein Kazemnejad, Milad Aghajohari, Eva Portelance, Alessandro Sordoni, Siva Reddy, Aaron Courville, and Nicolas Le Roux. Vineppo: Unlocking rl potential for llm reasoning through refined credit assignment. *arXiv preprint arXiv:2410.01679*, 2024.

Nathan Lambert, Jacob Morrison, Valentina Pyatkin, Shengyi Huang, Hamish Ivison, Faeze Brahman, Lester James V. Miranda, Alisa Liu, Nouha Dziri, Shane Lyu, Yuling Gu, Saumya Malik, Victoria Graf, Jena D. Hwang, Jiangjiang Yang, Ronan Le Bras, Oyvind Tafjord, Chris Wilhelm, Luca Soldaini, Noah A. Smith, Yizhong Wang, Pradeep Dasigi, and Hannaneh Hajishirzi. Tulu 3: Pushing frontiers in open language model post-training, 2025. URL <https://arxiv.org/abs/2411.15124>.

Aitor Lewkowycz, Anders Andreassen, David Dohan, Ethan Dyer, Henryk Michalewski, Vinay V. Ramasesh, Ambrose Sloane, Cem Anil, Imanol Schlag, Theo Gutman-Solo, Yuhuai Wu, Behnam Neyshabur, Guy Gur-Ari, and Vedant Misra. Solving quantitative reasoning problems with language models. In *NeurIPS*, 2022.

Jia Li, Edward Beeching, Lewis Tunstall, Ben Lipkin, Roman Soletskyi, Shengyi Huang, Kashif Rasul, Longhui Yu, Albert Q. Jiang, Ziju Shen, et al. Numinamath: The largest public dataset in ai4maths with 860k pairs of competition math problems and solutions. <https://huggingface.co/datasets/Numinamath>, 2024a. Hugging Face repository, 13:9.

Jinyang Li, Binyuan Hui, Ge Qu, Jiaxi Yang, Binhu Li, Bowen Li, Bailin Wang, Bowen Qin, Ruiying Geng, Nan Huo, et al. Can llm already serve as a database interface? a big bench for large-scale database grounded text-to-sqls. *Advances in Neural Information Processing Systems*, 36, 2024b.

Long Li, Xuzheng He, Haozhe Wang, Linlin Wang, and Liang He. How do humans write code? large models do it the same way too. In Yaser Al-Onaizan, Mohit Bansal, and Yun-Nung Chen (eds.), *Proceedings of the 2024 Conference on Empirical Methods in Natural Language Processing*, pp. 4638–4649, Miami, Florida, USA, November 2024c. Association for Computational Linguistics. doi: 10.18653/v1/2024.emnlp-main.267. URL <https://aclanthology.org/2024.emnlp-main.267/>.

Qingbin Li, Rongkun Xue, Jie Wang, Ming Zhou, Zhi Li, Xiaofeng Ji, Yongqi Wang, Miao Liu, Zheming Yang, Minghui Qiu, and Jing Yang. Cure: Critical-token-guided re-concatenation for entropy-collapse prevention, 2025. URL <https://arxiv.org/abs/2508.11016>.

Xiao Liang, Zhongzhi Li, Yeyun Gong, Yelong Shen, Ying Nian Wu, Zhijiang Guo, and Weizhu Chen. Beyond pass@1: Self-play with variational problem synthesis sustains rlvr, 2025. URL <https://arxiv.org/abs/2508.14029>.

Mingyang Liu, Gabriele Farina, and Asuman Ozdaglar. Uft: Unifying supervised and reinforcement fine-tuning, 2025a. URL <https://arxiv.org/abs/2505.16984>.

Zihan Liu, Zhuolin Yang, Yang Chen, Chankyu Lee, Mohammad Shoeybi, Bryan Catanzaro, and Wei Ping. Acereason-nemotron 1.1: Advancing math and code reasoning through sft and rl synergy, 2025b. URL <https://arxiv.org/abs/2506.13284>.

Ziru Liu, Cheng Gong, Xinyu Fu, Yaofang Liu, Ran Chen, Shoubo Hu, Suiyun Zhang, Rui Liu, Qingfu Zhang, and Dandan Tu. Ghpo: Adaptive guidance for stable and efficient llm reinforcement learning, 2025c. URL <https://arxiv.org/abs/2507.10628>.

Xingtai Lv, Yuxin Zuo, Youbang Sun, Hongyi Liu, Yuntian Wei, Zhekai Chen, Lixuan He, Xuekai Zhu, Kaiyan Zhang, Bingning Wang, Ning Ding, and Bowen Zhou. Towards a unified view of large language model post-training, 2025. URL <https://arxiv.org/abs/2509.04419>.

Sadegh Mahdavi, Muchen Li, Kaiwen Liu, Renjie Liao, and Christos Thrampoulidis. Beyond accuracy: A policy gradient reweighting approach for pass@ k maximization in llms. In *2nd AI for Math Workshop@ ICML 2025*.

Meta AI. Introducing meta Llama 3: The most capable openly available LLM to date, April 2024. URL <https://ai.meta.com/blog/meta-llama-3/>. Accessed: 2024-04-18.

MiniMax, :, Aili Chen, Aonian Li, Bangwei Gong, Binyang Jiang, Bo Fei, Bo Yang, Boji Shan, Changqing Yu, Chao Wang, Cheng Zhu, Chengjun Xiao, Chengyu Du, Chi Zhang, Chu Qiao, Chunhao Zhang, Chunhui Du, Congchao Guo, Da Chen, Deming Ding, Dianjun Sun, Dong Li, Enwei Jiao, Haigang Zhou, Haimo Zhang, Han Ding, Haohai Sun, Haoyu Feng, Huaiguang Cai, Haichao Zhu, Jian Sun, Jiaqi Zhuang, Jiaren Cai, Jiayuan Song, Jin Zhu, Jingyang Li, Jinhao Tian, Jinli Liu, Junhao Xu, Junjie Yan, Junteng Liu, Junxian He, Kaiyi Feng, Ke Yang, Kecheng Xiao, Le Han, Leyang Wang, Lianfei Yu, Liheng Feng, Lin Li, Lin Zheng, Linge Du, Lingyu Yang, Lunbin Zeng, Minghui Yu, Mingliang Tao, Mingyuan Chi, Mozhi Zhang, Mujie Lin, Nan Hu, Nongyu Di, Peng Gao, Pengfei Li, Pengyu Zhao, Qibing Ren, Qidi Xu, Qile Li, Qin Wang, Rong Tian, Ruitao Leng, Shaoxiang Chen, Shaoyu Chen, Shengmin Shi, Shitong Weng, Shuchang

Guan, Shuqi Yu, Sichen Li, Songquan Zhu, Tengfei Li, Tianchi Cai, Tianrun Liang, Weiyu Cheng, Weize Kong, Wenkai Li, Xiancai Chen, Xiangjun Song, Xiao Luo, Xiao Su, Xiaobo Li, Xiaodong Han, Xinzhu Hou, Xuan Lu, Xun Zou, Xuyang Shen, Yan Gong, Yan Ma, Yang Wang, Yiqi Shi, Yiran Zhong, Yonghong Duan, Yongxiang Fu, Yongyi Hu, Yu Gao, Yuanxiang Fan, Yufeng Yang, Yuhao Li, Yulin Hu, Yunan Huang, Yunji Li, Yunzhi Xu, Yuxin Mao, Yuxuan Shi, Yuze Wenren, Zehan Li, Zelin Li, Zhanxu Tian, Zhengmao Zhu, Zhenhua Fan, Zhenzhen Wu, Zhichao Xu, Zhihang Yu, Zhiheng Lyu, Zhuo Jiang, Zibo Gao, Zijia Wu, Zijian Song, and Zijun Sun. Minimax-m1: Scaling test-time compute efficiently with lightning attention, 2025. URL <https://arxiv.org/abs/2506.13585>.

OpenAI. GPT4 technical report. *arXiv preprint arXiv:2303.08774*, 2023.

OpenAI. Learning to reason with llms, 2024. URL <https://openai.com/index/learning-to-reason-with-llms/>.

Mihir Prabhudesai, Lili Chen, Alex Ippoliti, Katerina Fragkiadaki, Hao Liu, and Deepak Pathak. Maximizing confidence alone improves reasoning, 2025. URL <https://arxiv.org/abs/2505.22660>.

Qwen. Qwq-32b: Embracing the power of reinforcement learning, 2024. URL <https://qwenlm.github.io/blog/qwq-32b/>.

John Schulman, Sergey Levine, Pieter Abbeel, Michael Jordan, and Philipp Moritz. Trust region policy optimization. In *International conference on machine learning*, pp. 1889–1897. PMLR, 2015.

John Schulman, Filip Wolski, Prafulla Dhariwal, Alec Radford, and Oleg Klimov. Proximal policy optimization algorithms. *arXiv preprint arXiv:1707.06347*, 2017.

Zhihong Shao, Peiyi Wang, Qihao Zhu, Runxin Xu, Junxiao Song, Mingchuan Zhang, YK Li, Y Wu, and Daya Guo. Deepseekmath: Pushing the limits of mathematical reasoning in open language models. *arXiv preprint arXiv:2402.03300*, 2024.

Zhengyang Tang, Xingxing Zhang, Benyou Wang, and Furu Wei. Mathscales: scaling instruction tuning for mathematical reasoning. In *Proceedings of the 41st International Conference on Machine Learning*, ICML’24. JMLR.org, 2024.

Kimi Team, Angang Du, Bofei Gao, Bowei Xing, Changjiu Jiang, Cheng Chen, Cheng Li, Chenjun Xiao, Chenzhuang Du, Chonghua Liao, Chunling Tang, Congcong Wang, Dehao Zhang, Enming Yuan, Enzhe Lu, Fengxiang Tang, Flood Sung, Guangda Wei, Guokun Lai, Haiqing Guo, Han Zhu, Hao Ding, Hao Hu, Hao Yang, Hao Zhang, Haotian Yao, Haotian Zhao, Haoyu Lu, Haoze Li, Haozhen Yu, Hongcheng Gao, Huabin Zheng, Huan Yuan, Jia Chen, Jianhang Guo, Jianlin Su, Jianzhou Wang, Jie Zhao, Jin Zhang, Jingyuan Liu, Junjie Yan, Junyan Wu, Lidong Shi, Ling Ye, Longhui Yu, Mengnan Dong, Neo Zhang, Ningchen Ma, Qiwei Pan, Qucheng Gong, Shaowei Liu, Shengling Ma, Shupeng Wei, Sihan Cao, Siying Huang, Tao Jiang, Weihao Gao, Weimin Xiong, Weiran He, Weixiao Huang, Weixin Xu, Wenhao Wu, Wenyang He, Xianghui Wei, Xianqing Jia, Xingzhe Wu, Xinran Xu, Xinxing Zu, Xinyu Zhou, Xuehai Pan, Y. Charles, Yang Li, Yangyang Hu, Yangyang Liu, Yanru Chen, Yejie Wang, Yibo Liu, Yidao Qin, Yifeng Liu, Ying Yang, Yiping Bao, Yulun Du, Yuxin Wu, Yuzhi Wang, Zaida Zhou, Zhaoji Wang, Zhaowei Li, Zhen Zhu, Zheng Zhang, Zhexu Wang, Zhilin Yang, Zhiqi Huang, Zihao Huang, Ziyao Xu, Zonghan Yang, and Zongyu Lin. Kimi k1.5: Scaling reinforcement learning with llms, 2025. URL <https://arxiv.org/abs/2501.12599>.

Qwen Team. Qwen2.5: A party of foundation models, September 2024. URL <https://qwenlm.github.io/blog/qwen2.5/>.

Christian Walder and Deep Karkhanis. Pass@ k policy optimization: Solving harder reinforcement learning problems. *arXiv preprint arXiv:2505.15201*, 2025.

Chaoqi Wang, Yibo Jiang, Chenghao Yang, Han Liu, and Yuxin Chen. Beyond reverse kl: Generalizing direct preference optimization with diverse divergence constraints. In *The Twelfth International Conference on Learning Representations*.

Chaoqi Wang, Yibo Jiang, Chenghao Yang, Han Liu, and Yuxin Chen. Beyond reverse KL: Generalizing direct preference optimization with diverse divergence constraints. In *The Twelfth International Conference on Learning Representations*, 2024. URL <https://openreview.net/forum?id=2cRzmWXK9N>.

Guoqing Wang, Sunhao Dai, Guangze Ye, Zeyu Gan, Wei Yao, Yong Deng, Xiaofeng Wu, and Zhenzhe Ying. Information gain-based policy optimization: A simple and effective approach for multi-turn llm agents, 2025a. URL <https://arxiv.org/abs/2510.14967>.

Shenzhi Wang, Le Yu, Chang Gao, Chujie Zheng, Shixuan Liu, Rui Lu, Kai Dang, Xionghui Chen, Jianxin Yang, Zhenru Zhang, Yuqiong Liu, An Yang, Andrew Zhao, Yang Yue, Shiji Song, Bowen Yu, Gao Huang, and Junyang Lin. Beyond the 80/20 rule: High-entropy minority tokens drive effective reinforcement learning for llm reasoning, 2025b. URL <https://arxiv.org/abs/2506.01939>.

Jianhao Yan, Yafu Li, Zican Hu, Zhi Wang, Ganqu Cui, Xiaoye Qu, Yu Cheng, and Yue Zhang. Learning to reason under off-policy guidance, 2025. URL <https://arxiv.org/abs/2504.14945>.

An Yang, Anfeng Li, Baosong Yang, Beichen Zhang, Binyuan Hui, Bo Zheng, Bowen Yu, Chang Gao, Chengan Huang, Chenxu Lv, Chujie Zheng, Dayiheng Liu, Fan Zhou, Fei Huang, Feng Hu, Hao Ge, Haoran Wei, Huan Lin, Jialong Tang, Jian Yang, Jianhong Tu, Jianwei Zhang, Jianxin Yang, Jiaxi Yang, Jing Zhou, Jingren Zhou, Junyang Lin, Kai Dang, Keqin Bao, Kexin Yang, Le Yu, Lianghao Deng, Mei Li, Mingfeng Xue, Mingze Li, Pei Zhang, Peng Wang, Qin Zhu, Rui Men, Ruize Gao, Shixuan Liu, Shuang Luo, Tianhao Li, Tianyi Tang, Wenbiao Yin, Xingzhang Ren, Xinyu Wang, Xinyu Zhang, Xuancheng Ren, Yang Fan, Yang Su, Yichang Zhang, Yinger Zhang, Yu Wan, Yuqiong Liu, Zekun Wang, Zeyu Cui, Zhenru Zhang, Zhipeng Zhou, and Zihan Qiu. Qwen3 technical report, 2025. URL <https://arxiv.org/abs/2505.09388>.

Qiyi Yu, Zheng Zhang, Ruofei Zhu, Yufeng Yuan, Xiaochen Zuo, Yu Yue, Weinan Dai, Tiantian Fan, Gaohong Liu, Lingjun Liu, Xin Liu, Haibin Lin, Zhiqi Lin, Bole Ma, Guangming Sheng, Yuxuan Tong, Chi Zhang, Mofan Zhang, Wang Zhang, Hang Zhu, Jinhua Zhu, Jiaze Chen, Jiangjie Chen, Chengyi Wang, Hongli Yu, Yuxuan Song, Xiangpeng Wei, Hao Zhou, Jingjing Liu, Wei-Ying Ma, Ya-Qin Zhang, Lin Yan, Mu Qiao, Yonghui Wu, and Mingxuan Wang. Dapo: An open-source llm reinforcement learning system at scale, 2025. URL <https://arxiv.org/abs/2503.14476>.

Tao Yu, Rui Zhang, Kai Yang, Michihiro Yasunaga, Dongxu Wang, Zifan Li, James Ma, Irene Li, Qingning Yao, Shanelle Roman, et al. Spider: A large-scale human-labeled dataset for complex and cross-domain semantic parsing and text-to-sql task. In *Proceedings of the 2018 Conference on Empirical Methods in Natural Language Processing*, pp. 3911–3921, 2018.

Yang Yue, Zhiqi Chen, Rui Lu, Andrew Zhao, Zhaokai Wang, Yang Yue, Shiji Song, and Gao Huang. Does reinforcement learning really incentivize reasoning capacity in LLMs beyond the base model? In *2nd AI for Math Workshop @ ICML 2025*, 2025. URL <https://openreview.net/forum?id=upehLVgq1b>.

A THE USE OF LARGE LANGUAGE MODELS

In our work, we exclusively use LLMs for writing refinement, which means we first write a piece of text ourselves, and then use the LLM to correct grammar, formatting, and other issues. For our experiments, we also use LLMs to help us fix code bugs and generate Python code for plotting.

B MULTIPLE STYLE CAPABILITY EXPERIMENT

We construct a base model that outputs five different solution styles for SQL problems. This model is then used for reinforcement learning training. Next, we sample each question 32 times. Based on the output prefix, we count the number of times each distinct style appears within these 32 samples. For prefixes that are not among our original five styles (e.g., the model combines several different prefixes), we categorize them as “Others” and treat them as an additional style.

The result shows in Figure 2. On the base model, we find that it can fully output all styles. However, after training with reverse KL-constrained GRPO, most outputs degenerate into a single style. In contrast, forward KL significantly mitigates the degradation of the model’s ability to produce different styles.

C PRELIMINARIES ON f -DIVERGENCE

Table 5: Summary of some typical f-divergences $D_f(p\|q)$ together with their generator functions $f(u)$. In this paper, we let π_{ref} be q , and the formula for f-divergence references an improved version (Wang et al., 2024), the definitions for forward-KL and reverse-KL are swapped compared to Wikipedia. For all divergences, the generator function $f : \mathbb{R}^+ \rightarrow \mathbb{R} \cup \{+\infty\}$ is strictly convex, lower-semicontinuous, and satisfies $f(1) = 0$. Forward-KL and reverse-KL are the special case of alpha divergence.

| Name | Divergence Definition $D_f(p\ q)$ | Generator $f(u)$ |
|---|--|--|
| Reverse-KL($\alpha = 0$) | $\int p(x) \log \frac{p(x)}{q(x)} dx$ | $u \log u$ |
| Forward-KL($\alpha = 1$) | $\int q(x) \log \frac{q(x)}{p(x)} dx$ | $-\log u$ |
| α -divergence ($\alpha \notin \{0, 1\}$) | $\frac{1}{\alpha(\alpha-1)} \int q(x) \left[\left(\frac{p(x)}{q(x)} \right)^\alpha - \alpha \left(\frac{p(x)}{q(x)} \right) - 1 \right] dx$ | $(u^{1-\alpha} - (1-\alpha)u - \alpha)/(\alpha(\alpha-1))$ |
| Jensen-Shannon | $\frac{1}{2} \int \left(p(x) \log \frac{2p(x)}{p(x)+q(x)} + q(x) \log \frac{2q(x)}{p(x)+q(x)} \right) dx$ | $\frac{u}{2} \log u - \frac{(u+1)}{2} \log \frac{u+1}{2}$ |

D RLVR ALGORITHMS

D.1 GROUP RELATIVE POLICY OPTIMIZATION (GRPO)

GRPO presents an innovative approach to policy learning that distinguishes itself from methods like Proximal Policy Optimization (PPO) by eliminating the need for an explicit value function. Instead, GRPO computes the advantage in a group-relative manner, offering a streamlined yet effective optimization strategy.

For a specific question-answer pair (q, a) , GRPO’s underlying behavior policy, $\pi_{\theta_{\text{old}}}$, generates a group of G individual responses, denoted as $\{o_i\}_{i=1}^G$. The advantage for the i -th response within this

ensemble is then precisely calculated by normalizing the rewards specific to that group, $\{R_i\}_{i=1}^G$:

$$\hat{A}_{i,t} = \frac{r_i - \text{mean}(\{R_i\}_{i=1}^G)}{\text{std}(\{R_i\}_{i=1}^G)}. \quad (9)$$

Similar to the clipped surrogate objective found in PPO, GRPO also incorporates a clipping mechanism to constrain policy updates. This helps maintain training stability and improve sample efficiency by ensuring that new policies don't deviate too drastically from previous ones. Beyond this, GRPO further enhances regularization by directly adding a Kullback-Leibler (KL) divergence penalty term to its objective function. This penalty helps prevent the policy from drifting too far from a reference policy, promoting stable and controlled learning.

The comprehensive objective function for GRPO is articulated as:

$$\begin{aligned} \mathcal{L}_{\text{GRPO}}(\theta) = -\mathbb{E}_{\substack{(q,a) \sim \mathcal{D} \\ o_i \sim \pi_{\theta_{\text{old}}}(\cdot|q)}} \left[\frac{1}{G} \sum_{i=1}^G \frac{1}{|o_i|} \sum_{t=1}^{|o_i|} \left(\min \left(\rho_{i,t}(\theta) \hat{A}_{i,t}, \text{clip}(\rho_{i,t}(\theta), 1 - \varepsilon, 1 + \varepsilon) \hat{A}_{i,t} \right) \right. \right. \\ \left. \left. - \eta D_{\text{KL}}(\pi_{\theta} || \pi_{\text{ref}}) \right) \right], \end{aligned} \quad (10)$$

where η is a coefficient for the KL penalty, $D_{\text{KL}}(\pi_{\theta} || \pi_{\text{ref}})$ quantifies the KL divergence between the current policy π_{θ} and a specified reference policy π_{ref} . The term $\rho_{i,t}(\theta)$ represents the importance sampling ratio for the i -th response at time t , which is defined as:

$$\rho_{i,t}(\theta) = \frac{\pi_{\theta}(o_{i,t} | q, o_{i,<t})}{\pi_{\theta_{\text{old}}}(o_{i,t} | q, o_{i,<t})}. \quad (11)$$

A critical design choice in GRPO is its sample-level objective computation. Specifically, the loss is first averaged within each generated sequence, and subsequently, these sequence-level losses are averaged across various samples. This distinct computational approach, particularly when compared to token-level optimizations, can significantly influence the algorithm's empirical performance.

Traditional GRPO applies a single, unified loss function to all training samples. This loss includes a KL divergence penalty, typically in the form of reverse KL divergence, which aims to keep the fine-tuned policy close to the base policy. This penalty is added directly to the policy gradient loss. When applied to our experimental setup, the KL penalty for samples from \mathcal{D}_{exp} would be:

$$\mathcal{L}_{\text{KL-GRPO}} = \mathbb{E}_{q \sim \mathcal{D}_{\text{exp}}} [-\beta D_{\text{KL}}(\pi_{\theta} || \pi_{\text{base}})], \quad (12)$$

where the reverse KL divergence is defined as:

$$D_{\text{KL}}(\pi_{\theta} || \pi_{\text{base}}) = \sum_x \pi_{\theta}(x) \log \left(\frac{\pi_{\theta}(x)}{\pi_{\text{base}}(x)} \right). \quad (13)$$

Here, the term $D_{\text{KL}}(\pi_{\theta} || \pi_{\text{base}})$ represents the **Reverse KL Divergence**. It measures the information lost when the base policy π_{base} approximates the new policy π_{θ} . This choice heavily penalizes the new policy π_{θ} for exploring actions that the base policy π_{base} considers to have a low probability. In other words, if the new policy π_{θ} assigns a high probability to an action where the base policy π_{base} assigns a near-zero probability, this divergence will be very large. The effect is to strongly encourage the new policy π_{θ} to stick to the modes (high-probability regions) of the original base policy π_{base} , which restricts the exploration space.

D.2 DYNAMIC SAMPLING POLICY OPTIMIZATION (DAPO)

DAPO is an enhancement of the GRPO algorithm, incorporating several key improvements. DAPO eliminates the KL penalty and refines the clipping mechanism, changing the upper bound from $(1 + \varepsilon)$ to a fixed value of $(1 + \varepsilon_{\text{upper}})$, where $\varepsilon_{\text{upper}}$ is set to 0.28. A core innovation of DAPO is its dynamic sampling mechanism, which moves beyond the “all-or-nothing” approach to sampling. Additionally, the algorithm applies a token-level policy gradient loss and uses an overlong reward shaping technique.

E METHOD FOR DIVERGENCE DEFINITION

For f-divergences like forward KL, the Divergence Definition and Generator implementations are equivalent. However, for divergences such as JS divergence, which require sampling from both the reference policy π_{ref} and the new policy π_θ :

$$\text{JS}(\pi_{\text{base}} \parallel \pi_\theta) = \frac{1}{2} D_{\text{KL}} \left(\pi_{\text{base}} \parallel \frac{\pi_{\text{base}} + \pi_\theta}{2} \right) + \frac{1}{2} D_{\text{KL}} \left(\pi_\theta \parallel \frac{\pi_{\text{base}} + \pi_\theta}{2} \right) \quad (14)$$

Since the JS divergence is composed of two parts, we use data from the \mathcal{D}_{pef} loss to compute the first part $D_{\text{KL}} \left(\pi_{\text{base}} \parallel \frac{\pi_{\text{base}} + \pi_\theta}{2} \right)$. For the training on the \mathcal{D}_{exp} loss, we introduce a reference model to calculate the value of the second part $D_{\text{KL}} \left(\pi_\theta \parallel \frac{\pi_{\text{base}} + \pi_\theta}{2} \right)$.

The loss for DPH-JS on the \mathcal{D}_{exp} can be written as:

$$\begin{aligned} \mathcal{L}_{\text{DPH-exp}}(\theta) = -\mathbb{E}_{\substack{(q, a) \sim \mathcal{D}_{\text{exp}} \\ o_i \sim \pi_{\theta_{\text{old}}}(\cdot | q)}} \left[\frac{1}{G} \sum_{i=1}^G \frac{1}{|o_i|} \sum_{t=1}^{|o_i|} \min \left(\rho_{i,t}(\theta) \hat{A}_{i,t}, \text{clip}(\rho_{i,t}(\theta), 1 - \varepsilon, 1 + \varepsilon) \hat{A}_{i,t} \right) \right. \\ \left. - \beta_1 D_{\text{KL}} \left(\pi_\theta \parallel \frac{\pi_{\text{base}} + \pi_\theta}{2} \right) \right] \end{aligned} \quad (15)$$

By adjusting the value of β_1 , we can make the values of the two JS components within the same batch as close as possible, thereby achieving balance during training. β_1 is not a hyperparameter; it only depends on the dataset size and η . Its formula is:

$$\beta_1 = \eta * \frac{|\mathcal{D}_{\text{pef}}|}{|\mathcal{D}_{\text{exp}}|} \quad (16)$$

The loss for DPH-JS on the \mathcal{D}_{pef} can be expressed as:

$$\mathcal{L}_{\text{DPH-pef}} = \mathbb{E}_{q \sim \mathcal{D}_{\text{pef}}} \left[D_{\text{KL}} \left(\pi_{\text{base}} \parallel \frac{\pi_{\text{base}} + \pi_\theta}{2} \right) \right] \quad (17)$$

F TRAINING DETAILS

F.1 TASK SETTINGS

For the SQL task, we used the Llama-3.1-8B-Instruct and OmniSQL32B models. We performed RL training exclusively on the BIRD dataset Li et al. (2024b) and then evaluated the models on both the BIRD and Spider (Cross-Domain) Yu et al. (2018) datasets. To validate the generalization of our method, we also tested it on a mathematical reasoning task, treating it as an out-of-domain (OOD) evaluation.

For the mathematical reasoning task, we used the Llama-3.1-8B-Instruct and Qwen2.5-Math-7B models. We conducted RL training on a DAPO-17K subset, having first filtered out problems that initially had a Pass@8 score of 0. For testing, we used seven different datasets: AIME24 Li et al. (2024a), AIME25, AMC23 Li et al. (2024a), Math500 Hendrycks et al. (2021), Olympiad He et al. (2024), Minerva Lewkowycz et al. (2022), and College Math Tang et al. (2024).

Evaluation For the SQL tasks, the model will generate an SQL statement, and then we call the SQL executor to get the result. This result is typically a tuple, such as $[(\text{string}, \text{int}), (\text{string}, \text{int})]$. We compute the Cartesian product of the prediction and the ground truth. For the math tasks, we use the official Qwen2.5 evaluation tool¹ for a detailed assessment, as this tool provides tailored evaluations for each dataset.

F.2 METHOD SETTINGS

The implementation of RKL is consistent with the standard GRPO implementation. Our default implementation for DPH-RL uses the **Generator** method. The settings for our different methods

¹<https://github.com/QwenLM/Qwen2.5-Math>

Table 6: Configuration Comparison of RL Methods

| Method | Online Data | Offline Data | Offline Loss | η | ϵ_{high} | Dynamic Sampling |
|----------------------|--|----------------------------|----------------------|--------|--------------------------|------------------|
| GRPO | $\mathcal{D}_{\text{exp}}, \mathcal{D}_{\text{pef}}$ | - | - | - | 0.2 | \times |
| DAPO | $\mathcal{D}_{\text{exp}}, \mathcal{D}_{\text{pef}}$ | - | - | - | 0.28 | \checkmark |
| RKL | $\mathcal{D}_{\text{exp}}, \mathcal{D}_{\text{pef}}$ | - | - | 0.01 | 0.28 | \checkmark |
| α -divergence | \mathcal{D}_{exp} | \mathcal{D}_{pef} | α -divergence | 0.01 | 0.28 | \checkmark |
| DPH-F | \mathcal{D}_{exp} | \mathcal{D}_{pef} | Forward KL | 0.01 | 0.28 | \checkmark |
| DPH-JS | \mathcal{D}_{exp} | \mathcal{D}_{pef} | JS divergence | 0.2 | 0.28 | \checkmark |

are detailed in Table 6. For all RL algorithms, we consistently use a token-level loss. In most of our experiments, the ϵ_{high} for our DPH methods was set to 0.28. However, due to training instability in the Llama math experiments, we set the ϵ_{high} to 0.2 for all methods.

F.3 HYPERPARAMETERS

Table 7: Hyperparameters for RL Training

| Hyperparameter | Llama-SQL | OmniSQL-32B-SQL | Llama-Math | Qwen2.5-Math |
|------------------------------------|-----------|-----------------|------------|--------------|
| Batch Size | 128 | 128 | 128 | 128 |
| Learning Rate | 1e-6 | 1e-6 | 2e-7 | 2e-7 |
| Rollout Temperature | 1.0 | 1.0 | 1.0 | 1.0 |
| Rollout Top-p | 0.95 | 0.95 | 0.95 | 0.95 |
| Validation Temperature | 1.0 | 1.0 | 0.6 | 0.6 |
| Validation Top-p | 0.95 | 0.95 | 0.95 | 0.95 |
| PPO Epochs | 1 | 1 | 1 | 1 |
| Size of \mathcal{D}_{exp} | 6710 | 5169 | 4599 | 7009 |
| Size of \mathcal{D}_{pef} | 2248 | 3789 | 1248 | 3199 |
| Max Response Length | 4096 | 4096 | 2048 | 2048 |
| Number of Rollouts | 16 | 16 | 16 | 16 |
| Training Epochs | 4 | 4 | 8 | 8 |

All experiments were conducted on 32 NVIDIA A800-80G GPUs using the VeRL framework for our RL algorithm implementations. For all experiments, we set the number of rollouts to 16. In our setup, the training batch size was 128, and the batch size for the \mathcal{D}_{pef} data was 256. This resulted in using 2048 samples from \mathcal{D}_{exp} and 256 samples from \mathcal{D}_{pef} at each learning step, yielding an effective ratio of 8:1. A comprehensive list of the specific hyperparameters used is provided in Table 7.

In the offline phase, we used the current model to perform 8 rollouts on the training data. For the SQL tasks, we separated the perfectly correct examples from the rollouts and used the remaining ones to construct \mathcal{D}_{exp} . For the DAPO-17k dataset used in the math tasks, we discarded all data where the model’s responses were entirely incorrect.

G ADDITIONAL EXPERIMENTS

G.1 ERROR BAR

G.2 MEAN@K METRIC FOR MATHEMATICAL REASONING TASK

To verify that our reinforcement learning training was effective on the math tasks, we evaluated the performance using the mean@k metric in Table 8.

H CASE STUDY

We have listed the use cases and prompts for the two tasks in detail to facilitate future reproduction.

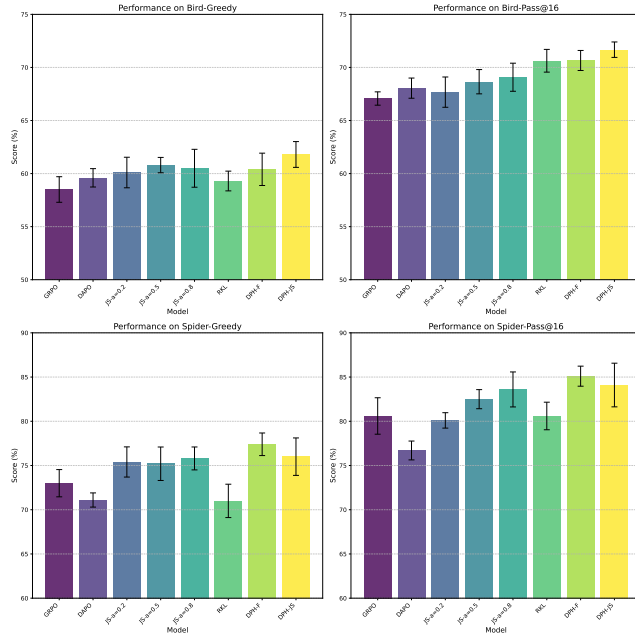


Figure 6: Error bar in Llama Sql. For each method in our Llama SQL experiments, we conducted three separate reinforcement learning training runs. We then selected the model that achieved the highest pass@16 score on the Bird.

Table 8: The Mean@k metric for models trained on math datasets. To accelerate training, we filtered the DAPO-17k dataset for data with a Pass@8 score of 0. In the end, we trained Llama on 5.8k samples and Qwen on 10.2k samples.

| Model | Mean@64 | | | Mean@16 | | | Mean@8 | Avg |
|------------------------------|---------|--------|-------|---------|----------|---------|--------------|-------|
| | AIME24 | AIME25 | AMC23 | Math500 | Olympiad | Minerva | College Math | |
| Llama-3.1-8B-Instruct | | | | | | | | |
| Base Model | 5.5 | 0.5 | 23.0 | 46.5 | 15.2 | 22.1 | 27.3 | 20.01 |
| RL Models | | | | | | | | |
| -GRPO | 5.6 | 0.6 | 23.3 | 47.7 | 14.9 | 25.4 | 29.1 | 20.94 |
| -RKL | 6.4 | 0.2 | 22.3 | 45.6 | 13.0 | 24.8 | 28.6 | 20.13 |
| -DPH-F | 6.2 | 0.5 | 23.8 | 48.1 | 15.5 | 25.4 | 29.7 | 21.31 |
| -DPH-JS | 8.4 | 0.5 | 24.2 | 48.4 | 15.6 | 27.4 | 29.9 | 22.06 |
| Qwen2.5-Math-7B | | | | | | | | |
| Base Model | 12.7 | 6.6 | 32.2 | 48.9 | 22.8 | 13.3 | 19.3 | 22.26 |
| RL Models | | | | | | | | |
| -GRPO | 25.8 | 10.9 | 60.6 | 75.5 | 37.8 | 38.8 | 40.6 | 41.43 |
| -DAPO | 25.9 | 11.1 | 61.3 | 76.3 | 37.6 | 39.0 | 40.7 | 41.70 |
| -RKL | 25.8 | 10.3 | 61.5 | 75.3 | 36.7 | 34.6 | 39.9 | 40.59 |
| -DPH-F | 26.0 | 10.6 | 60.4 | 76.4 | 37.3 | 38.1 | 40.9 | 41.38 |
| -DPH-JS | 26.6 | 11.2 | 62.7 | 76.5 | 38.5 | 38.9 | 41.9 | 42.33 |

H.1 SQL TASK

Case Study-SQL

System Prompt

You are Qwen, created by Alibaba Cloud. You are a helpful assistant.

User Prompt

Task Overview:

You are a data science expert. Below, you are provided with a database schema and a natural language question. Your task is to understand the schema and generate a valid SQL query to answer the question.

Database Engine:

SQLite

Database Schema:

```
CREATE TABLE frpm (
CDSCode text, – example: ['01100170109835', '01100170112607']
‘Academic Year‘ text, – example: ['2014-2015']
‘County Code‘ text, – example: ['01', '02']
‘Free Meal Count (K-12)‘ real, – example: [565.0, 186.0]
‘Percent (%) Eligible Free (K-12)‘ real, – example: [0.519779208831647,
0.470886075949367]
‘2013-14 CALPADS Fall 1 Certification Status‘ integer, – example: [1]
PRIMARY KEY (CDSCode),
CONSTRAINT fk_frpm_cdscode FOREIGN KEY (CDSCode) REFERENCES schools
(CDSCode)
);
```

CREATE TABLE.... This schema describes the database’s structure, including tables, columns, primary keys, foreign keys, and any relevant relationships or constraints.

Question:

Eligible free rate for K-12 = ‘Free Meal Count (K-12)‘ / ‘Enrollment (K-12)‘. What is the highest eligible free rate for K-12 students in the schools in Alameda County?

Instructions:

- Make sure you only output the information that is asked in the question. If the question asks for a specific column, make sure to only include that column in the SELECT clause, nothing more.
- The generated query should return all of the information asked in the question without any missing or extra information.
- Before generating the final SQL query, please think through the steps of how to write the query.

Output Format:

In your answer, please enclose the generated SQL query in a code block:

```
```sql
-- Your SQL query
```
```

Take a deep breath and think step by step to find the correct SQL query.

Response

To find the codes of the schools with a total enrollment of over 500, we need to follow these steps:

1. Identify the table that contains the enrollment data: The ‘frpm‘ table contains the ‘Enrollment (K-12)‘ and ‘Enrollment (Ages 5-17)‘ columns, which represent the enrollment data.
2. Identify the relevant columns: We need to sum the ‘Enrollment (K-12)‘ and ‘Enrollment (Ages 5-17)‘ columns to get the total enrollment.
3. Identify the filter condition: We need to filter the schools with a total enrollment of over 500.
4. Write the SQL query: We can use a ‘SELECT‘ statement to retrieve the ‘CDSCode‘ column from the ‘frpm‘ table, filtering the schools where the sum of ‘Enrollment (K-12)‘ and ‘Enrollment (Ages 5-17)‘ is greater than 500.

Based on these steps, the SQL query to find the codes of the schools with a total enrollment of over 500 is:

```
```sql
SELECT frpm.CDSCode
FROM frpm
```

---

```
WHERE frpm.'Enrollment (K-12)' + frpm.
 'Enrollment (Ages 5-17)' > 500;
 ``;
```

This query sums the 'Enrollment (K-12)' and 'Enrollment (Ages 5-17)' columns and filters the schools with a total enrollment of over 500, returning the 'CDSCode' column.

Execution results

```
[['01100170109835'], ['01100170112607'], ['01100170124172']]
```

## H.2 MATH TASK

### Case Study-Math

System Prompt

Please reason step by step, and put your final answer within \boxed{\{\}}.

User Prompt

Every morning Aya goes for a 9-kilometer-long walk and stops at a coffee shop afterwards. When she walks at a constant speed of  $s$  kilometers per hour, the walk takes her 4 hours, including  $t$  minutes spent in the coffee shop. When she walks  $s + 2$  kilometers per hour, the walk takes her 2 hours and 24 minutes, including  $t$  minutes spent in the coffee shop. Suppose Aya walks at  $s + \frac{1}{2}$  kilometers per hour. Find the number of minutes the walk takes her, including the  $t$  minutes spent in the coffee shop.

Response

To solve this problem, we need to first determine the value of  $s$  and  $t$ . We know the following:

1. When Aya walks at  $s$  km/h, the total time including the coffee shop visit is 4 hours.
2. When Aya walks at  $s + 2$  km/h, the total time including the coffee shop visit is 2 hours and 24 minutes (which is 2.4 hours).

First, we can set up the equations for the walking times:

1. For the first scenario:

$$\frac{9}{s} + \frac{t}{60} = 4$$

2. For the second scenario:

$$\frac{9}{s+2} + \frac{t}{60} = 2.4$$

We can solve these equations to find  $s$  and  $t$ .

Let's subtract the second equation from the first to eliminate  $t$ :

$$\frac{9}{s} - \frac{9}{s+2} = 1.6$$

This simplifies to:

$$\frac{9(s+2) - 9s}{s(s+2)} = 1.6$$

$$\frac{18}{s(s+2)} = 1.6$$

$$18 = 1.6s(s+2)$$

$$18 = 1.6s^2 + 3.2s$$

$$1.6s^2 + 3.2s - 18 = 0$$

We can solve this quadratic equation using the quadratic formula  $s = \frac{-b \pm \sqrt{b^2 - 4ac}}{2a}$ , where  $a = 1.6$ ,  $b = 3.2$ , and  $c = -18$ :

$$s = \frac{-3.2 \pm \sqrt{3.2^2 - 4 \cdot 1.6 \cdot (-18)}}{2 \cdot 1.6}$$

$$s = \frac{-3.2 \pm \sqrt{10.24 + 115.2}}{3.2}$$

$$s = \frac{-3.2 \pm \sqrt{125.44}}{3.2}$$

$$s = \frac{-3.2 \pm 11.2}{3.2}$$

This gives us two possible solutions:

$$s = \frac{8}{3.2} = 2.5 \quad (\text{positive root})$$

$$s = \frac{-14.4}{3.2} = -4.5 \quad (\text{negative root, not physically meaningful})$$

So,  $s = 2.5$  km/h. Now we can substitute  $s$  back into one of the original equations to find  $t$ :

$$\frac{9}{2.5} + \frac{t}{60} = 4$$

$$3.6 + \frac{t}{60} = 4$$

$$\frac{t}{60} = 0.4$$

$$t = 24$$

So,  $t = 24$  minutes. Now we need to find out how long the walk takes when Aya walks at  $s + \frac{1}{2} = 2.5 + 0.5 = 3$  km/h. The total time including the coffee shop visit will be:

$$\frac{9}{3} + \frac{24}{60} = 3 + 0.4 = 3.4 \text{ hours}$$

Converting 3.4 hours to minutes, we get:

$$3.4 \times 60 = 204 \text{ minutes}$$

So the final answer is 204.

---

## I PROOF OF THEOREM 1

The proof of Theorem 1 relies on bounding the total variation distance by various f-divergences. The following lemma, which is a direct consequence of the well-known Pinsker's inequality and its generalizations, establishes these relationships.

**Lemma 1.** *For any two probability distributions  $P$  and  $Q$  defined on the same measurable space, the squared total variation distance,  $D_{TV}^2(P, Q)$ , is bounded by the Kullback-Leibler (KL),  $\alpha$ -, and Jensen-Shannon (JS) divergences as follows:*

$$D_{TV}^2(P, Q) \leq C \cdot D_f(P \| Q)$$

where  $D_f$  is one of the specified divergences and  $C$  is a positive constant that depends on the choice of  $f$ .

*Proof.* The proof consists of recalling the standard Pinsker-type inequalities (Fedotov et al., 2003) for each specified f-divergence and arranging them into the desired form. We define the total variation distance as  $D_{TV}(P, Q) = \frac{1}{2} \sum_x |P(x) - Q(x)|$ .

- **Kullback-Leibler (KL) Divergence:** The classical Pinsker's inequality states that

$$D_{KL}(P \| Q) \geq 2D_{TV}^2(P, Q).$$

Rearranging this directly yields the desired bound:

$$D_{TV}^2(P, Q) \leq \frac{1}{2} D_{KL}(P \| Q).$$

Here,  $C = 1/2$ .

- **$\alpha$ -Divergence:** The relationship depends on the value of  $\alpha$ .

- For  $\alpha > 1$ , the  $\alpha$ -divergence is lower-bounded by the KL divergence. Consequently, the same constant applies:

$$D_\alpha(P \| Q) \geq D_{KL}(P \| Q) \geq 2D_{TV}^2(P, Q) \implies D_{TV}^2(P, Q) \leq \frac{1}{2} D_\alpha(P \| Q).$$

- For  $\alpha \in (0, 1)$ , a similar quadratic bound holds, of the form  $D_\alpha(P \| Q) \geq C_\alpha D_{TV}^2(P, Q)$  for some constant  $C_\alpha > 0$ . For instance, the Hellinger distance, which corresponds to  $\alpha = 1/2$  (up to a factor), satisfies  $H^2(P, Q) \geq 2D_{TV}^2(P, Q)$ .

In all cases, a suitable constant  $C$  exists.

- **Jensen-Shannon (JS) Divergence:** For the JS divergence, there are two well-known lower bounds of this form.

A commonly used quadratic inequality is:

$$D_{JS}(P \| Q) \geq \frac{1}{8} V(P, Q)^2$$

The tightest possible bound overall is non-quadratic:

$$D_{JS}(P \| Q) \geq \ln(2) - H_2\left(\frac{1 + V(P, Q)}{2}\right)$$

where  $H_2(p) = -p \ln(p) - (1-p) \ln(1-p)$ . This provides the sharpest possible function for  $g(V)$ .

Thus, for each of the considered f-divergences, we have established the existence of a constant  $C$  that satisfies the inequality. This concludes the proof. □

Throughout the following proof, we will repeatedly apply the lemma established in Schulman et al. (2015).

---

**Lemma 2** (Schulman et al. (2015)). *Given two policies  $\pi$  and  $\tilde{\pi}$ , we have*

$$J(\tilde{\pi}) - J(\pi) = \mathbb{E}_{\tau \sim \tilde{\pi}} \left[ \sum_{t=0}^{\infty} \gamma^t A_{\pi}(s_t, a_t) \right],$$

where the expectation is over the trajectories  $\tau := (s_0, a_0, s_1, a_1, \dots)$  and the notion  $\mathbb{E}$  indicates that  $\tau$  are sampled from  $\tilde{\pi}$  to generate  $\tau$ .

Given that  $\pi, \tilde{\pi}$  are  $\alpha$ -coupled policies, define  $A^{\tilde{\pi}|\pi}(s) = \mathbb{E}_{\tilde{a} \sim \tilde{\pi}} A_{\pi}(s, \tilde{a})$  we have following result.

**Lemma 3** (Lemma 4 in Kang et al. (2018)). *let  $(\pi, \tilde{\pi})$  be an  $\alpha$  - coupled policy pair. Then*

$$|\mathbb{E}_{s_t \sim \tilde{\pi}} [A^{\tilde{\pi}|\pi}(s_t)]| \leq 2\alpha(1 - (1 - \alpha)^t) \max_{s,a} |A_{\pi}(s, a)|$$

Now we are ready to prove our theorem 1.

*Proof.* Let's assume that the policy pairs  $(\pi, \tilde{\pi})$  and  $(\pi_{pef}, \tilde{\pi})$  are  $\alpha$ -coupled and  $\beta$ -coupled, respectively. This can be established if their total variation distances are bounded, i.e.,  $D_{TV}(\pi, \tilde{\pi}) \leq \alpha$  and  $D_{TV}(\pi_{pef}, \tilde{\pi}) \leq \beta$ . Our goal is to find a lower bound for the performance improvement  $J(\tilde{\pi}) - L_{\pi}(\tilde{\pi})$ . We proceed as follows:

$$\begin{aligned}
& J(\tilde{\pi}) - L_{\pi}(\tilde{\pi}) \\
& \stackrel{a}{=} \mathbb{E}_{s_t \sim \tilde{\pi}} \left[ \sum_{t=0}^{\infty} \gamma^t A^{\tilde{\pi}|\pi}(s_t) \right] - \mathbb{E}_{s_t \sim \pi} \left[ \sum_{t=0}^{\infty} \gamma^t A^{\tilde{\pi}|\pi}(s_t) \right] \\
& = \sum_{t=0}^{\infty} \left( \mathbb{E}_{s_t \sim \tilde{\pi}} [\gamma^t A^{\tilde{\pi}|\pi}(s_t)] - \mathbb{E}_{s_t \sim \pi_{pef}} [\gamma^t A^{\pi_{pef}|\pi}(s_t)] + \mathbb{E}_{s_t \sim \pi_{pef}} [\gamma^t A^{\pi_{pef}|\pi}(s_t)] - \mathbb{E}_{s_t \sim \pi} [\gamma^t A^{\tilde{\pi}|\pi}(s_t)] \right) \\
& \stackrel{b}{=} (\eta(\tilde{\pi}) - \eta(\pi)) - (\eta(\pi_{pef}) - \eta(\pi)) + \mathbb{E}_{s_t \sim \pi_{pef}} [\gamma^t A^{\pi_{pef}|\pi}(s_t)] - \mathbb{E}_{s_t \sim \pi} [\gamma^t A^{\tilde{\pi}|\pi}(s_t)] \\
& = \eta(\tilde{\pi}) - \eta(\pi_{pef}) + \mathbb{E}_{s_t \sim \pi_{pef}} [\gamma^t A^{\pi_{pef}|\pi}(s_t)] - \mathbb{E}_{s_t \sim \pi} [\gamma^t A^{\tilde{\pi}|\pi}(s_t)] \\
& \stackrel{c}{=} \sum_{t=0}^{\infty} \left( \mathbb{E}_{s_t \sim \tilde{\pi}} [\gamma^t A^{\tilde{\pi}|\pi_{pef}}(s_t)] + \mathbb{E}_{s_t \sim \pi_{pef}} [\gamma^t A^{\pi_{pef}|\pi}(s_t)] - \mathbb{E}_{s_t \sim \pi} [\gamma^t A^{\tilde{\pi}|\pi}(s_t)] \right) \\
& \stackrel{d}{\geq} \sum_{t=0}^{\infty} \left( -2\gamma^t \beta (1 - (1 - \beta)^t) \max_{(s,a)} |A_{\pi_{pef}}(s, a)| + \gamma^t \delta - 2\gamma^t \alpha (1 - (1 - \alpha)^t) \max_{(s,a)} |A_{\pi}(s, a)| \right) \\
& = -\frac{2\beta^2 \gamma \epsilon_p}{(1 - \gamma)(1 - \gamma(1 - \beta))} - \frac{2\alpha^2 \gamma \epsilon_{\pi}}{(1 - \gamma)(1 - \gamma(1 - \alpha))} + \frac{\delta}{1 - \gamma} \\
& \geq -\frac{2\gamma(\beta^2 \epsilon_p + \alpha^2 \epsilon_{\pi})}{(1 - \gamma)^2} + \frac{\delta}{1 - \gamma}
\end{aligned} \tag{18}$$

where equality  $a, b, c$  holds from Lemma 2; inequality  $d$  applies Lemma 3.

The final result is obtained by using the fact that  $(1 - \gamma(1 - x)) > (1 - \gamma)$  for  $x \in (0, 1)$ , which simplifies the denominator.

The theorem's full statement is established by using Lemma 1 to connect the KL-divergence bounds to the total variation distances ( $D_{TV}$ ), which in turn provides the conditions for the policy pairs to be  $\alpha$ -coupled and  $\beta$ -coupled.

□